Hindawi
Wireless Communications and Mobile Computing
Volume 2022, Article ID 8676849, 9 pages
https://doi.org/10.1155/2022/8676849

WILEY | Hindawi

Research Article

Research on Towed Linear Array Shape Measurement Method Based on Biorthogonal Signal

Sen Zhang, Ming-Zhi Wang, Jun Yuan, and Chen-Lin Zhou

School of Electronic Engineering, Naval University of Engineering, Wuhan 430033, China

Correspondence should be addressed to Sen Zhang; johnson_xh@sina.com

Received 20 January 2022; Revised 15 March 2022; Accepted 18 March 2022; Published 20 April 2022

Academic Editor: Hamada Esmaiel

Systematic error and random error are main factors affecting the positioning of biorthogonal signal underwater positioning system. Based on the operation theory of USBL, this paper quantitatively analyzes a theoretical analysis and simulation calculations on influence of different error sources on the positioning accuracy and qualitatively analyzes the effectiveness of the towed linear array shape measurement method based on biorthogonal signal through practical experiments. By comparing the measurement effect after correction by using the measurement array with the measurement effect based on the linear array, the effectiveness of the method is verified.

1. Introduction

With the development of marine resources, underwater acoustic positioning and navigation system have received extensive attention and research. According to the length of array, it can be divided into long baseline LBL, short baseline SBL, and ultrashort baseline USBL [1]. This kind of underwater acoustic navigation and positioning system is very similar to the radio navigation system with the shore radio beacon as the reference point. The distance between the two sides is determined by measuring the phase difference and time delay between the reference point and the moving carrier, and then, the position of the moving carrier is calculated to realize the function of navigation and positioning. The advantages of long baseline are high positioning accuracy and long operating distance, but the disadvantages are high cost and difficult to place and recover. The short baseline is longer, and the positioning accuracy and operating distance of the baseline are poor, so the cost is reduced. The ultrashort baseline array has small size and convenient installation [2].

Based on the principle of ultrashort baseline positioning system, this paper analyzes the research on towed linear array shape measurement method based on biorthogonal signal, which mainly measures the influence of positioning error under different array element radius, depth error caused by pressure sensor, attitude angle error caused by attitude sensor, and signal-to-noise ratio error in random error on positioning accuracy. This paper quantitatively analyzes a theoretical analysis and simulation calculations on influence of different error sources on the positioning accuracy and qualitatively analyzes the effectiveness of the towed linear array shape measurement method based on biorthogonal signal through practical experiments. By comparing the measurement effect after correction by using the measurement array with the measurement effect based on the linear array, the effectiveness of the method is verified.

2. Working Principle

The system consists of transmitting terminal and receiving terminal. The transmitting terminal consists of two transmitting transducers connected by rigid connection and two transmitting transducers to launch different orthogonal signal at the same time; a receiving transducer is used as the receiver to receive the two signals, by processing the separation and obtaining the time delay between the signal and phase difference. Thus, the azimuth of the receiver relative to the transmitter is obtained. Then, measure the distance between the transmitting terminal and the receiving terminal (the depth difference between the transmitting terminal

and the receiving terminal can be obtained with the help of the depth sensor), and the position of the receiving terminal relative to the transmitting terminal can be obtained.

Set A and B as two transmitting array, take the connecting line between them as the x-axis, the midpoint between them as the origin O, and the vertical downward as the z-axis, and establish the coordinate system as shown in Figure 1. T is the target terminal, and $[x, y, z]$ is its coordinates. The receiver terminal T with the launch of the distance between A and B, respectively, is R_A and R_B, the distance between the origin O, and the target terminal T is R. The angle between attachment OT and X axis is α, and the angle between the ABT plane and the XOY plane is β [3–5].

Assuming that the located target end meets the far-field assumption conditions, then:

$$\cos\alpha = \frac{R_{BA}}{L} = \frac{t_{BA}c}{L}, \tag{1}$$

where L is the interval between the array elements, d is the radius of the element, $R_{BA} = R_B - R_A$ is the range difference between the two transmitting terminal and the positioning target terminal T, t_{BA} is the corresponding propagation time difference, and c is the sound speed. The coordinates of the targeted terminal T are as follows:

$$\begin{cases} x = R\cos\alpha, \\ y = R\sin\alpha\cos\beta, \\ z = R\sin\alpha\sin\beta. \end{cases} \tag{2}$$

When t is the propagation time of acoustic wave propagating from the origin O to the targeted terminal T, then $R = c * t$; at this point, the x-axis coordinate of t point is

$$x = R\cos\alpha = c^2 t\frac{t_{BA}}{2d}. \tag{3}$$

The depth z of the target terminal to be located is measured by the depth sensor, set $z = D$, and then:

$$\sin\beta = \frac{D}{R\sin\alpha}. \tag{4}$$

After simplification, the coordinate value of T can be solved:

$$\begin{cases} x = c^2 t\frac{t_{BA}}{2d}, \\ y = \sqrt{c^2t^2 - x^2 - D^2}, \\ z = D. \end{cases} \tag{5}$$

According to trigonometry, the distance between the target terminal and the origin of coordinates can be expressed as follows:

$$R = \frac{1}{2}\sqrt{2{R_A}^2 + 2{R_B}^2 - 4d^2}. \tag{6}$$

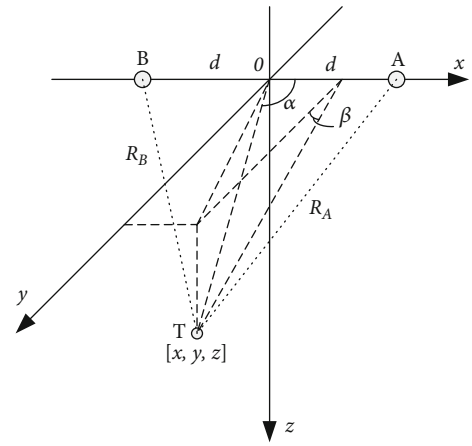

Figure 1: Principle of ranging and positioning.

At this point, the propagation delay can be expressed as follows:

$$t = \frac{R}{c} = \frac{1}{2}\sqrt{2{t_A}^2 + 2{t_B}^2 - \frac{4d^2}{c^2}}. \tag{7}$$

3. System Composition

The system consists of transmitter and receiver, as shown in Figure 2. The transmitter is located on the towed body and consists of transducer array, transmitter subsystem, and attitude measurement subsystem. The receiving terminal is located on the ship and consists of towed line array subsystem and receiving and processing subsystem. The time synchronization between the transmitter and the receiver is realized by the synchronization clock module [3].

3.1. Control and Processing Center. The control and processing center mainly performs the following functions: (1) receive PPS and UTC clock data output by GPS receiver, synchronize with internal thermostatic crystal oscillator, and maintains its own time; (2) read the attitude sensor data, add the time stamp, and save it; (3) generate two channel phase coded signals and output them to the power amplifier; and (4) the attitude sensor data and temperature and depth sensor data stored in the control center can be read externally through Ethernet.

3.2. Power Amplifier. The power amplifier mainly performs the following functions: (1) power amplification of the transmitted signal generated by the signal source; and (2) complete the impedance matching with the transmitting transducer.

3.3. Transmitting Transducer Array. The transmitting terminal is composed of two transmitting transducers through rigid connection, and the two transmitting transducers simultaneously emit different orthogonal signals.

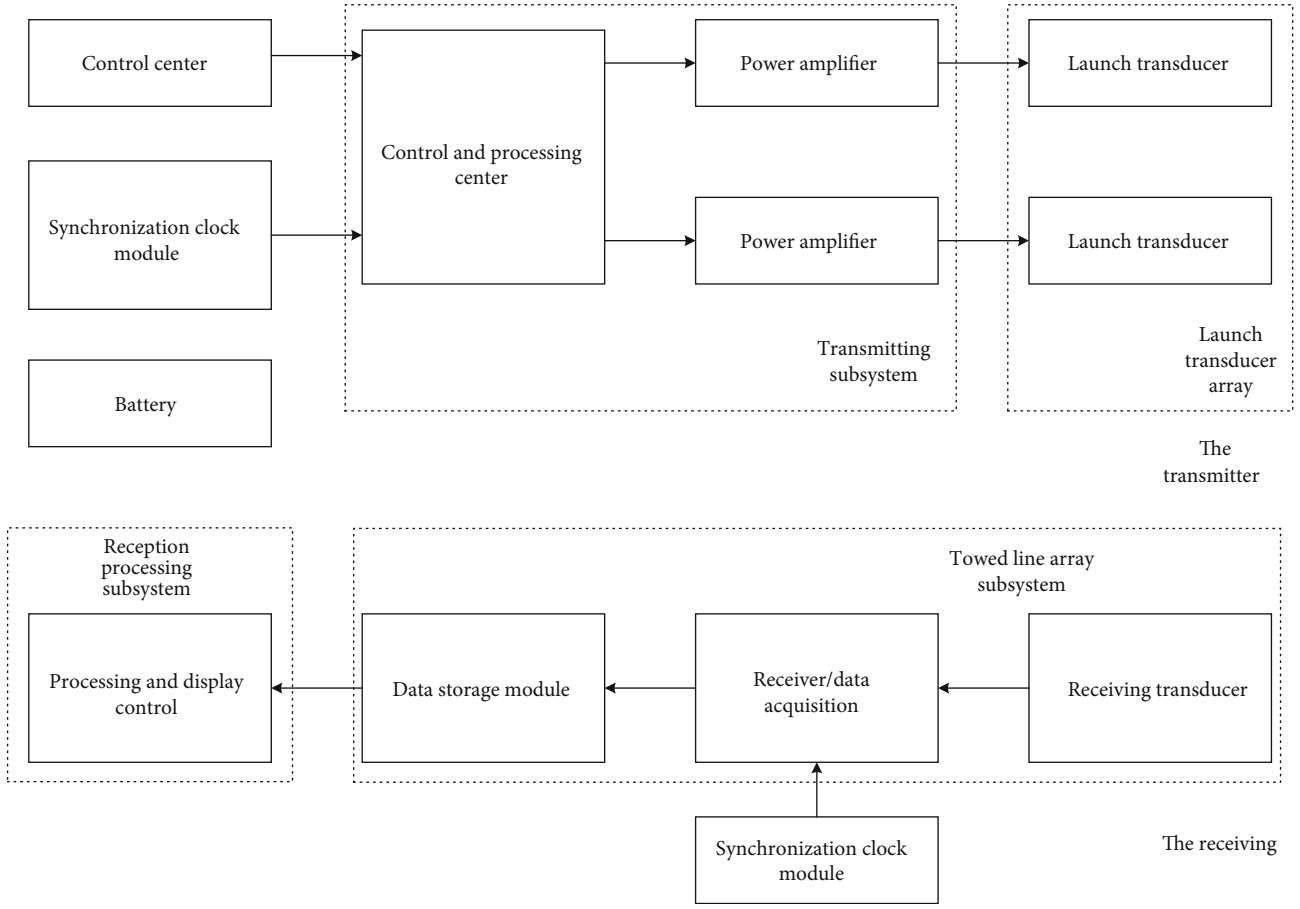

Figure 2: Schematic diagram of transmitter and receiver.

3.4. Receiving Terminal. The receiver terminal amplifies and filters the received weak electrical signal. The synchronization clock generates the trigger clock at the agreed time (i.e., the launch time), which triggers the data acquisition unit to start collecting. The data acquisition module converts analog signals into digital signals and sends them to the data storage module for storage. The data storage module contains gigabit Ethernet ports. After being reclaimed, the data stored on the data storage module is read through gigabit Ethernet ports and processed offline.

4. Positioning Error Analysis

4.1. System Error. Systematic error is caused by factors that are fixed or change according to a certain law. Under the same measurement conditions, this law can be repeated and expressed by functions or curves in principle.

Firstly, the positioning error in the horizontal direction is analyzed and obtained from Equation (3):

$$x = c^2 t \frac{t_{BA}}{2d}, \tag{8}$$

where t is the propagation delay from the transmitting terminal to the receiving terminal and the synchronous ranging method is adopted in this paper and is the one-way time difference. Let us differentiate both sides completely,

$$\Delta x = \frac{ctt_{BA}}{d}\Delta c + \frac{c^2 t_{BA}}{2d}\Delta t + \frac{c^2 t}{2d}\Delta t_{BA} - \frac{c^2 t t_{BA}}{2d^2}\Delta d. \tag{9}$$

Similarly, the positioning error of the y-axis can be obtained:

$$\begin{aligned}\Delta y = {} & \frac{ct^2\Delta c}{\sqrt{c^2t^2 - x^2 - D^2}} + \frac{c^2 t\Delta t}{\sqrt{c^2t^2 - x^2 - D^2}} \\ & - \frac{x\Delta x}{\sqrt{c^2t^2 - x^2 - D^2}} - \frac{D\Delta D}{\sqrt{c^2t^2 - x^2 - D^2}}.\end{aligned} \tag{10}$$

The depth information D of z-axis can be obtained from the pressure sensor:

$$\Delta z = \Delta D. \tag{11}$$

As for the positioning of the receiving terminal, the total position error is caused by the errors in the three directions of x-axis, y-axis, and z-axis, so the relative deviation is

$$\frac{\Delta P}{R} = \sqrt{\left(\frac{\Delta x}{R}\right)^2 + \left(\frac{\Delta y}{R}\right)^2 + \left(\frac{\Delta z}{R}\right)^2}. \quad (12)$$

According to Equations (9)–(12), the main error sources are sound velocity error, delay measurement error, array element radius error, and depth measurement error caused by array installation.

After the array is installed and fixed, the radius error caused by the array installation can be ignored. At present, the sound velocity error can usually be controlled within 0.1% distance, so it has little influence. However, the phase measurement error caused by sound bending depends on the sound velocity structure in the operation area and is mainly caused by the temperature density change of water in the sound propagation path [6, 7]. In the simulation experiment, it is assumed that the sound velocity is constant, which is 1500 m/s. According to Equations (9)–(12), the larger the radius of the array element is, the smaller the mean square positioning error is. However, the radius of the array element should be controlled according to the actual needs. The depth error generated by the pressure sensor can be seen from Equation (11), which will have an impact on the positioning error, mainly determined by the performance parameters of the pressure sensor.

In addition to acoustic positioning errors, joint transmitter attitude information is required in the conversion to the geodetic coordinate system. The attitude angle error generated by the attitude sensor causes the deviation of the array coordinate system, which need to be converted into actual coordinates through the rotation matrix, as shown in the following formula [8–10]:

$$P = \begin{bmatrix} \cos\theta & -\sin\theta & 0 \\ \sin\theta & \cos\theta & 0 \\ 0 & 0 & 1 \end{bmatrix}^{-1} [x^* \; y^* \; z^*]. \quad (13)$$

In Equation (13), P is the actual coordinate, α is the attitude angle error, and $[x^*, y^*, z^*]$ is the measured coordinate without attitude angle error. The change of attitude angle error will affect the positioning error.

4.2. Random Error. The random error mainly includes delay measurement error and phase measurement error caused by noise. The timing error consists of clock error and pulse front measurement error. The clock error is very small and can not be considered. The measurement error of pulse front is caused by ocean noise and related to SNR.

Δt, the error caused by time delay measurement, and as can be known from signal detection and estimation knowledge, the time delay measurement error through correlation processing is

$$\Delta t \approx \frac{1}{2\pi f_0 \sqrt{BT}\sqrt{SNR}}, \quad (14)$$

where B is the transmitted signal bandwidth (Hz), SNR is the signal-to-noise ratio, and T is the duration. Since acoustic wave propagation can be regarded as spherical expansion, SNR approximation is inversely proportional to the square of the distance under the condition of constant transmitting power; then, $\sqrt{SNR}$ approximation is inversely proportional to the distance. Δt can be approximately regarded as proportional to distance change, while $1/t$ is inversely proportional to distance change. The combination of the two can approximately offset the error effect caused by propagation loss in distance variation. Therefore, the error of time delay measurement is mainly determined by the center frequency of the system. The farther the distance is, the greater the error is (SNR decreases due to the propagation loss). At present, the relative error of experimental measurement can be controlled within 0.1%, so the influence is not significant [10].

For the phase measurement error, the optimality of the estimated value can be determined by using the Cramer-Rao lower bound:

$$\Delta\varphi \approx \frac{1}{\sqrt{SNR}}. \quad (15)$$

It can be seen from Equation (15) that the phase measurement error is inversely proportional to the square root of SNR. The effective method to improve the phase measurement accuracy is to improve SNR. It is more advantageous to use lower frequency and broadband signal. Therefore, the greater the noise in the propagation process of underwater acoustic signal, the greater the random error of measurement. Improving SNR can effectively reduce the influence of ocean noise on measurement results and improve the performance of the whole system.

In this paper, the experimental system error mainly considers the array radius error caused by the array installation, the depth error caused by the pressure sensor, and the attitude angle error caused by the attitude sensor.

5. Simulation Analysis of Positioning Error

In this section, the influence of different error sources on positioning accuracy was compared by simulation. The MATLAB 2016a software was used for simulation. The specific simulation environment was $z = 300$ m at the receiving terminal, SNR was 20 dB, and the influence on positioning accuracy of the system when the array element radius changed within the range of 0.5-3 m was considered. We used Monte Carlo method to calculate the radius error of each element 100 times. When the receiver was at different positions (100,600) and (200,600), the mean square positioning error changed with the radius of array element, as shown in Figure 3.

Considering the influence of attitude angle error on positioning accuracy of the system when it varied within 0-0.2°, when the receiver was at different positions (100,600) and (200,600), the change of the mean square positioning error with attitude angle error was shown in Figure 4.

Considering that the depth measurement error z varies between 0 and 0.1 m, when the receiving terminal is at different depths, namely, $z = 300$ m and $z = 500$ m, the change of

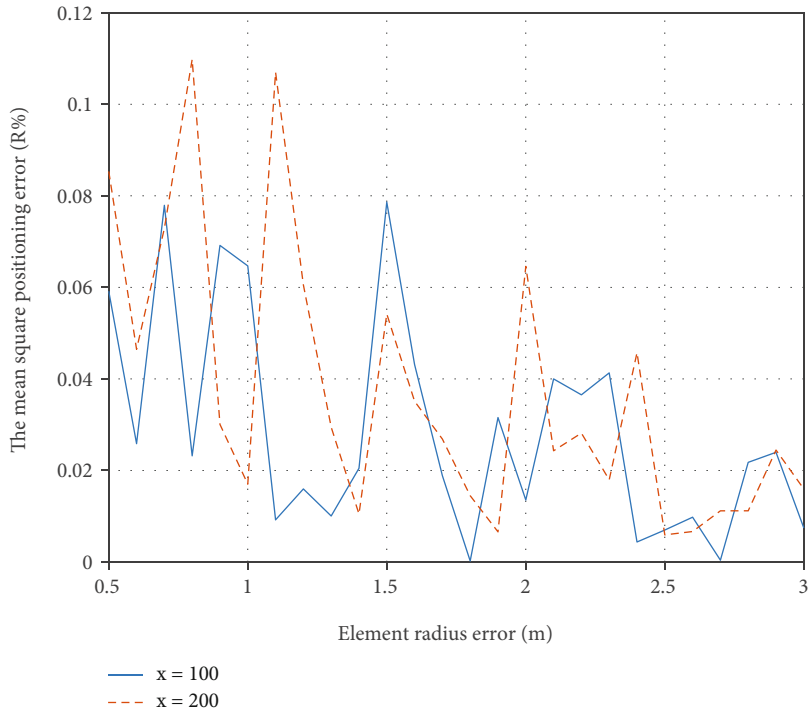

Figure 3: Element radius error.

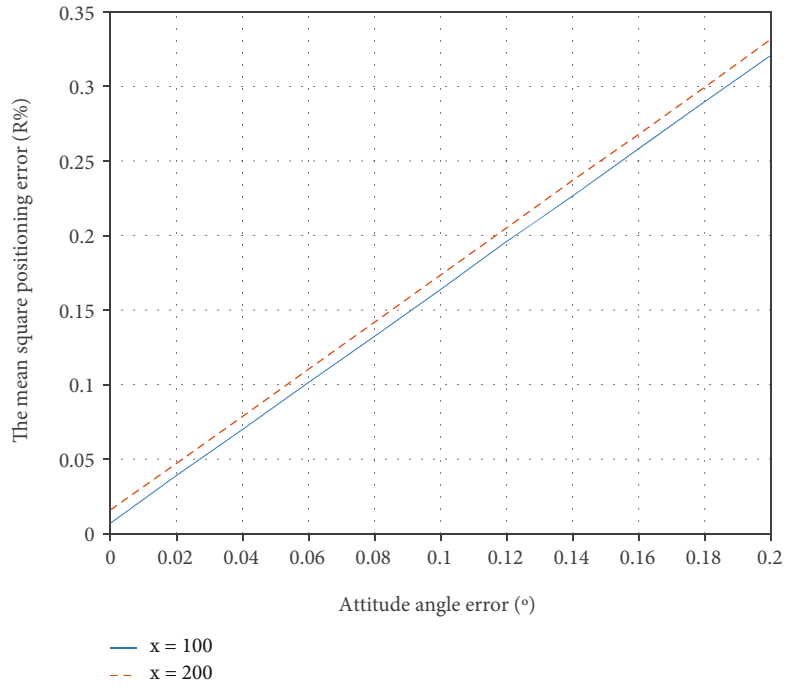

Figure 4: Attitude angle error.

the mean square positioning error with depth measurement error is shown in Figure 5.

Similarly, when the SNR error varies within the range of -5-20 dB, the influence on the positioning accuracy of the system is considered. When the receiver is at different positions (100,600) and (200,600), the change of the mean square positioning error with the SNR error is shown in Figure 6.

As shown in Figure 3, in the general trend, the mean square positioning error gradually decreases as the radius error of array element increases, and the error is less than 0.1%. Due to the influence of signal coherence, the error will

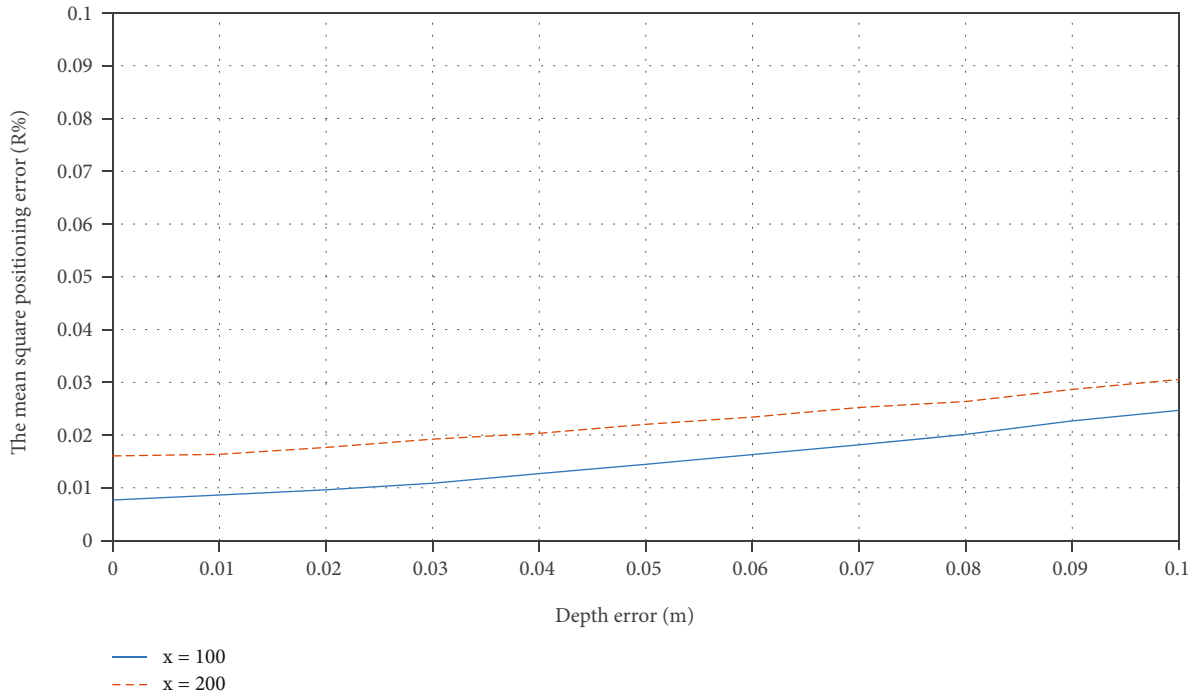

Figure 5: Depth error.

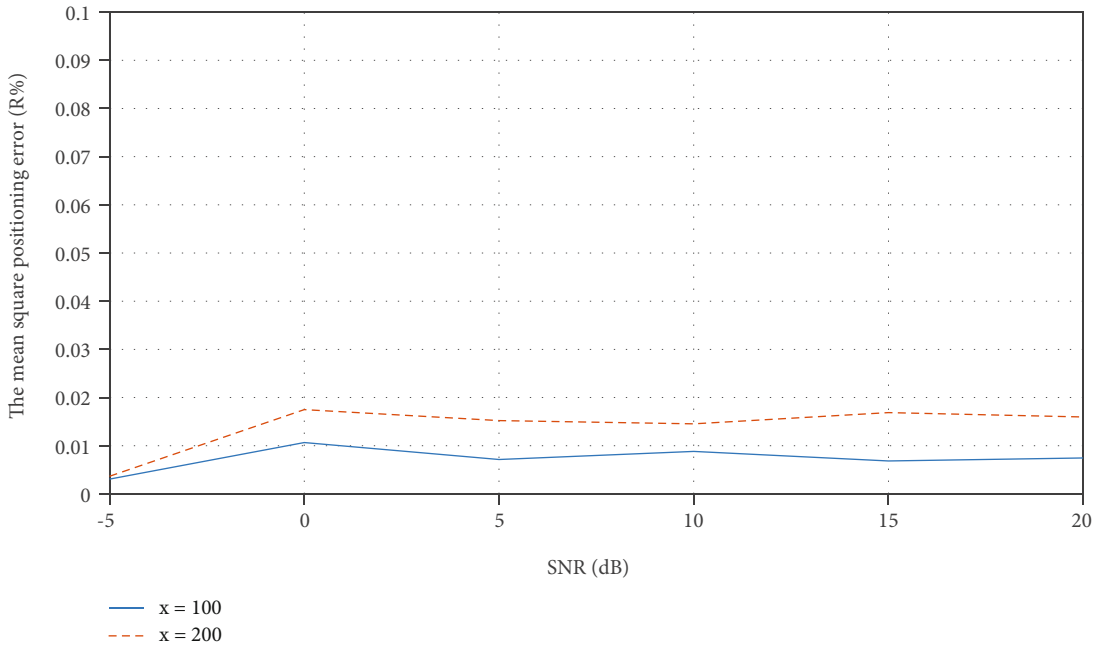

Figure 6: SNR error.

show certain ups and downs when the receiver is at different positions. As shown in Figure 4, the mean square positioning error increases with the increase of attitude angle error, showing an approximate linear relationship. As shown in Figure 5, the mean square positioning error increases as the depth measurement error increases, and the mean square positioning error does not exceed 0.03%. As shown in Figure 6, the mean square positioning error tends to be stable with the increase of SNR. The main reason is that the positioning signals are multiple orthogonal signals with large time broadband and wide product. At a certain SNR, the cross-correlation sidelobe level signal is higher than the noise signal after matched filtering, so the change of SNR has little influence on the positioning error.

Table 1: Towed body roll angle and inclination angle data.

	Amount of data	Average	Standard deviation	Minimum value	Median	Maximum
Inclination angle	205153	5.21631	1.06777	8.63	5.36	0.94
Roll angle	205153	1.1049	0.40981	0.56	1.09	2.7

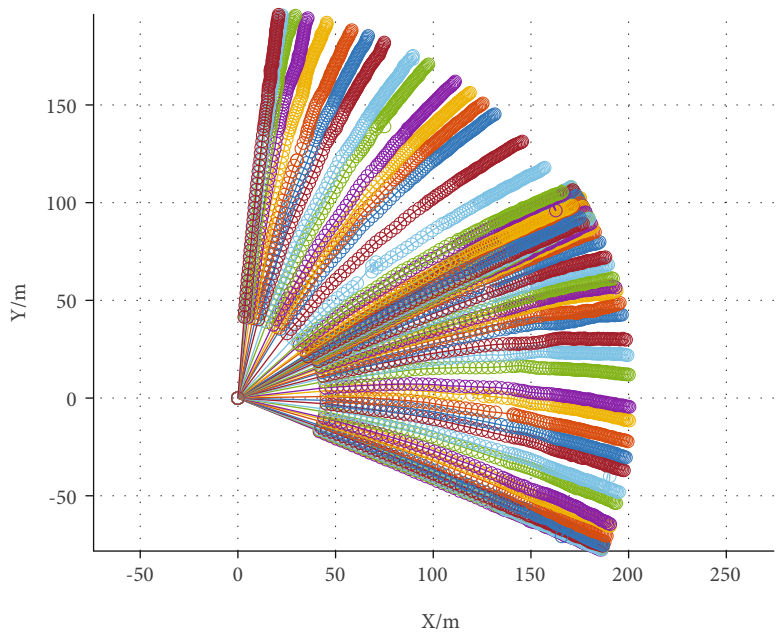

Figure 7: Formation measurement results during sea test.

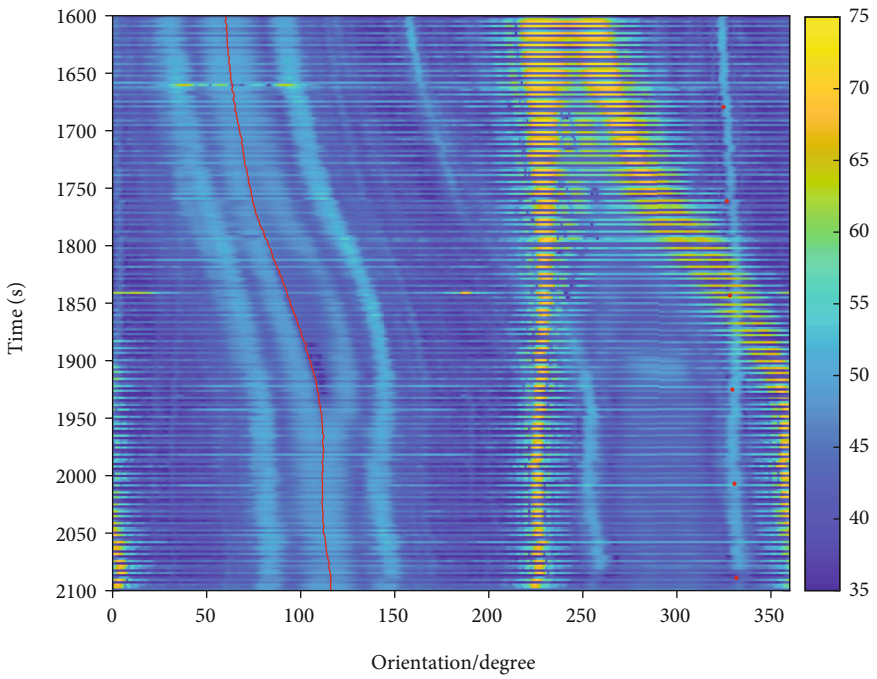

Figure 8: Process diagram after array correction by measuring array.

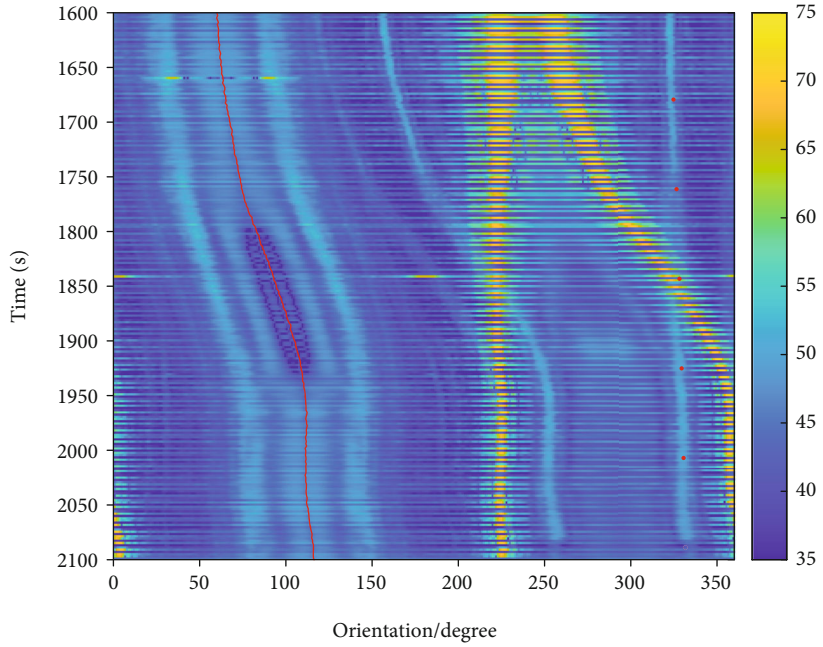

Figure 9: Process diagram based on linear array.

6. Positioning Test Certificate

In April 2021, sea trials were carried out in the South China Sea in four stages: launching of the towed vehicle, operation stability test of towed vehicle under different ship speed, operation stability test of towed body and receiving array cable, and measurement test of towed line array under maneuvering steering condition of towed body cable.

The test of the towed body under the condition of maneuvering steering of the cable was conducted for 348 minutes in total. After entering the water for 20 minutes, the towed body gradually dived to a depth of 27 m and continued to run at a depth of about 27 m for about 130 min. The heading gradually changed from 180° to about 0°. From the 150th minute, the dive reached a depth of about 35~40 m, and the operation lasted for 200 min. The heading gradually changed from 0° to -180°, completing a circle. In the stable operation stage, the roll angle and inclination angle of the towed body changed in a small range, as shown in Table 1.

During the sea test in South China Sea, the measurement formation was shown in Figure 7 during the turning process.

It can be seen from Figure 7 that the spacing of array elements is obviously different, which is consistent with the actual situation. At the same time, it can be clearly seen that the dragging array turns from the left side of the array to the right side of the array during the steering process, which is consistent with the dragging state.

It can be seen from Figures 8 and 9 that the red line is the heading of the towboat, which turns from 58° to 113° (about 50°) within 500 s. The red point is the heading of the target ship measured by GPS. As shown in Figure 9, when using linear array for beamforming, the heading course of the target is blurred and divergent. As shown in Figure 8, after correction, the target is more concentrated and can achieve accurate and steady direction finding in the process of turning.

7. Conclusion

To sum up, the error of attitude sensor has a great impact on the measurement accuracy and limit the positioning accuracy of the system. At present, the heading measurement error of the fiber optic inertial navigation sensor is usually about 0.1°, so the overall positioning accuracy is about 0.2% slant distance. At the same time, the experiment proves that the technique of using orthogonal signal to measure the formation is feasible, which can measure the position of each element of the line array effectively in the state of dragging.

The experiment still has the following deficiencies:

(1) In the actual experiment in the South China Sea, due to the difficulty of controlling different influence sources, the effectiveness of the experiment can only be qualitatively analyzed by comparing the measurement effect after correction by using the measurement array with the measurement effect based on the linear array. The influence of different error sources on positioning accuracy is quantitatively analyzed through simulation experiments

(2) In order to measure real-time data, we need to install a measuring device on the towed cable, so it will have an impact on the layout and salvage process of the towed cable

We will continue to improve relevant experiments in the follow-up work.

Data Availability

The equipment data used to support the findings of this study have not been made available because the equipment data belongs to the confidentiality requirements of Naval University of engineering, Wuhan.

Conflicts of Interest

The authors declare that they have no conflicts of interest.

References

[1] T. Jiang, "Analysis and simulation of positioning error in ultra-short baseline positioning system," *Mine Warfare & Ship Self-Defence*, vol. 4, 2012.

[2] Y. Han, C. Zheng, and D. Sun, "A high precision calibration method for long baseline acoustic positioning systems," *Chinese Journal of Acoustics*, vol. 4, pp. 489–500, 2017.

[3] S. Zhang, J. Guo, and Z. Tian, "An underwater navigation system based on multi-orthogonal signals and its lake trial," in *2017 IEEE 17th International Conference on Communication Technology (ICCT).*, Chengdu, China, 2017.

[4] S. Zhang, J. Guo, and W. U. Yuanyuan, "Calibration algorithm for underwater navigation system based on Rodrigues matrix transformation," *Acta Armamentarii*, vol. 41, no. 2, p. 8, 2020.

[5] J. Guo and S. Zhang, "Research on CRLB for position calibration of underwater navigation system with multiple orthogonal signals," *Ship Electronic Engineering*, vol. 39, no. 4, p. 5, 2019.

[6] Q. H. Tang, Y. T. Wu, J. S. Ding, L. Yang, and Y. X. Liu, "Calibration of ultra-short baseline acoustic positioning system," *Technical Acoustics*, vol. 25, 2006.

[7] C. H. Tian, "Error analysis and experiment of USBL positioning," *Journal of Waterway and Harbor*, vol. 36, 2015.

[8] H. C. Sui, C. H. Tian, D. Z. Han, and C. M. Wang, "Error analysis of underwater positioning system," *Journal of Waterway & Harbor*, vol. 31, 2010.

[9] S. L. Zhang, "Applied of Rodrigues matrix on rigorous solution to collinear equation," *Journal of Wuhan Technical University of Surveying and Mapping*, vol. 1, pp. 81–91, 1987.

[10] W. U. Yuanyuan, S. Zhang, and J. Guo, "Calibration algorithm of underwater navigation system based on Gauss-Newton algorithm," *Ship Electronic Engineering*, vol. 38, no. 11, 2018.